Vol 25, No.2 (2024)

http://www.veterinaria.org

Article Received: Revised: Published:



# "Biogenic Synthesis Of Silver Nanoparticles Using porphyra Indica & Gracilaria Salicornia: Chemical And Pharmacological Potentials And Applications"

## Malikka.B<sup>1\*</sup>, Yokeswari Nithya P<sup>2</sup>

<sup>1\*</sup>Research Scholar (Reg-21212012032001), PG& Research Department of chemistry, A.P.C Mahalaxmi College for women, Thoothukudi, Affiliated to Manonmaniam sundaranar University, Abishekapatti, Tirunelveli-627012, Tamilnadu, India

<sup>2</sup>Assistant Professor of Chemistry, PG & Research Department of Chemistry, A.P.C. Mahalaxmi College for Women, Thoothukudi. Affiliated to Manonmaniam Sundaranar University, Abishekapatti, Tirunelveli-627012, Tamilnadu, India.

#### Abstract

Nanotechnology is making significant strides in agriculture, feed, and food technology, yet biosynthesis of silver oxide nanoparticles (Ag<sub>2</sub>O NPs) remains underexplored. In this study, Ag<sub>2</sub>O NPs were synthesized using red algae species *Porphyra indica* and *Gracilaria salicornia*, and their antibiofilm and electrochemical properties were evaluated. The UV-visible spectrum revealed characteristic absorption peaks at 280 nm and 290 nm. X-ray diffraction analysis confirmed the face-centered cubic crystalline structure of Ag<sub>2</sub>O NPs, with a narrow peak indicating high crystallinity. High-resolution Transmission Electron Microscopy (HR-TEM) revealed nanotube and cubic morphologies, ranging from 7.71 to 7.86 nm in diameter. Fourier transform infrared spectroscopy (FTIR) identified functional groups corresponding to metabolites in the algae supernatant. The biosynthesized silver oxide nanoparticles (Ag<sub>2</sub>O NPs) demonstrated significant antibacterial activity against marine biofilm-forming bacteria and several common pathogenic strains, including *Escherichia coli*, *Staphylococcus aureus*, *Bacillus subtilis*, *Bacillus cereus*, and *Pseudomonas aeruginosa*. This was confirmed through observations made using confocal laser scanning microscopy (CLSM). Additionally, the Ag<sub>2</sub>O NPs demonstrated enhanced electrochemical sensing properties, particularly for physiological pH detection. This study underscores the potential of Ag<sub>2</sub>O NPs in antibacterial applications and electrochemical technologies.

Keywords: Antibacterial; Electro chemical analysis; Biosynthesis; Silver oxide nanoparticles

#### 1.Introduction

Natural sources such as plants, fungi, bacteria, and marine organisms have historically been a rich reservoir of bioactive compounds, including antibiotics. These natural products often possess unique chemical structures and mechanisms of action, making them promising candidates for drug discovery. (Wang et al., 2018). Nanoscale substances, such as nanoparticles and nanomaterials, exhibit unique properties that can enhance their antimicrobial activity. These properties include high surface area-to-volume ratios, increased reactivity, and the ability to penetrate microbial biofilms. Nanoparticles can directly interact with pathogens, disrupting their cellular structures or interfering with essential biological processes, thereby exerting potent antimicrobial effects. (Shanmuganathan et al., 2018).

Among the nanomaterials, metal nanoparticles (NPs) give the maximum effective outcome. Currently, several NPs for instance Ag, Ag2O, Au, Cu, CuO, CeO2, Fe, FeO, TiO2 and ZnO are synthesized via several methods, The choice of synthesis method influences the size, shape, and surface properties of the nanoparticles, which in turn affect their physicochemical properties and performance in different applications. Ongoing research continues to explore novel metal nanoparticles and optimize their properties for specific applications, driving innovation in nanotechnology and materials science. (Schröfel et al., 2014; Aiswarya Devi et al., 2017; Pugazhendhi et al., 2018). However, the application of NPs was limited in real-time usages, such as clinical, environmental remediation/reclamation, water treatment material, etc., (Kahru and Dubourguier, 2010). AgO NPs show a pronounced antibacterial activity not only against various pathogens, silver nanoparticles (Ag NPs) have garnered significant attention in the biomedical field due to their unique properties and versatile applications (Franci. G. et al., 2015: Vardanyan, Z et al., 2015)

Electrochemical methods were commonly accepted as the fastest analytical assay compared with traditional spectroscopic (Gurunathan, S et al.,2014).In order to increase the sensitivity and selectivity, various oxides such as CuO, ZnO, Mg2Fe2O4, CdO, NiO/ZnO hybrid nanoparticles modified carbon paste electrodes are reported (J. M. Zen et al.,2003; S. Reddy et al.,2012; S. Reddy et al.,2011; S. Reddy et al.,2010).With the terrestrial resources being greatly explored and exploited, researchers turn to the oceans for numerous reasons. The oceans cover more than 70% of the world surface housing 34 living phyla out of the 36 and more than 300,000 known species of fauna and flora. The marine environment is known to contain over 80% of world's plant and animal species. In recent years, many bioactive compounds have been extracted from various marine plants, marine animals and marine organisms .

Vol 25, No.2 (2024)

http://www.veterinaria.org

Article Received: Revised: Published:



Seaweeds are marine plants because they use the sun's energy to produce carbohydrates from carbon dioxide and water. In India seaweeds are mainly exploited by industries for phycocolloids but very poorly explored for their beneficial application in pharmacology . Seaweeds are important sources of protein, iodine, vitamins, minerals and poly phenols with their metabolites showing wide range of promising biological activities. Over the past several decades, seaweeds and their extracts have generated an enormous amount of interest in the pharmaceutical industry as a fresh source of bioactive compounds with immense medicinal potential. The macro algae reported to contain various significant compounds with anti bacterial, antiviral and antitumor activity. AgO-NPs have been synthesized using marine microalgae and screened for its antibacterial activity (J. Saraniya Devi and B. Valentin Bhimba.,2012).

Thereby, the present investigation was aimed at to find out the efficiency of marine red algae *Porphyra indica* (*Bangiaceae*) and *Gracilaria salicornia*(*Gracilariaceae*) .seaweedsextract in reduction of the toxic compound silver nitrate (AgNO<sub>3</sub>) into silver nanoparticles. The synthesized particles were characterized by severalspectroscopy. The obtained results show that silver nanoparticle /carbon paste electrode act as good electrochemical sensor for detection of UA in presence DA. In addition, there is a great need of finding new antibacterial agents against various pathogenic bacteria which causes some infectious diseases. Here prepared silver nanoparticles accomplish the need and acts as a promising antibacterial activity.

#### 2.Materials and Methods

*Porphyra indica* and *Gracilaria Salicornia* seaweeds were collected from coastal area,Rameswaram, India. Fresh seaweeds were rinsed using sterile sea water to remove epiphytes, salt, sand, microorganisms and other suspended materials associated with seaweeds.

#### 2.1. Preparation of seaweeds sample for experimental studies

The collected whole seaweeds were cut into small fragments and shade dried until the fraction is uniform and smooth. The dried seaweeds were cut and added to 5 ml of sterile seawater and dried. The sample materials were granulated or powdered by using a blender and sieved to get uniform particles by using sieve No. 60. The final uniform powder of the seaweeds was used for various experimental studies.

#### **Preparation of seaweed extracts**

Powdered *Porphyra indica* and *Gracilaria Salicornia* seaweeds (30 g) each were soaked separately in the organic solvents, viz. absolute ethanol gently mixed by shaking and kept at room temperature (28–30 °C) for three days. The crude extracts were filtered, and the residue was re-extracted in the same solvents for three days. The filtered crude extracts obtained were pooled and concentrated. The crude extracts obtained were weighed to determine extract yield and stored in the dark at 4 °C for further use. Stock solutions of seaweed extracts were further uses. (Afrin, F et al., 2023)

## 2.2 Synthesis of Silver oxide nanoparticles

For the synthesis of  $Ag_2O$ -NPs, 1 mM silver nitrate ( $Ag_2O$ -NPs) solution served as the silver ion source, and 20 g of aqueous seaweed extracts from *Porphyra indica* and *Gracilariasalicornia* were used as reducing mediators. A volume of 25 mL of seaweed extract (pH 6.0) was gradually added to 75 mL of  $AgNO_3$  solution over 15–20 minutes at 35  $\pm$  2 °C, with continuous stirring using a magnetic stirrer. The formation of  $Ag_2O$ -NPs was indicated by a color change from colourless to brown. The nanoparticles were then centrifuged at 12,000 rpm for 20 minutes, washed three times and dried at  $100 \pm 2$  °C. The dried nanoparticles were stored in a hermetically sealed container for future use (Harshiny Muthukumar et all.,2021).

#### 2.3 Characterization of Ag<sub>2</sub>O-NPs

The optical absorption of the  $Ag_2O$ -NPs was measured by UV–Vis spectroscopy . Presence of silver compound in the  $Ag_2O$ -NPs was identified using Scanning Electron micrography, Energy Dispersive spectroscopy. The bio-molecules of the *P.indica* extract ,*G.salicornia* extract and  $Ag_2O$ -NPs were identified by Fourier transform infrared spectroscopy (FTIR, Perkin-Elmer (IRAffinity-1S)). To determine crystalline nature of  $Ag_2O$ -NPs, X-ray powder diffraction studies was performed (XPERT-Pro diffractometer using Cu-Ka radiation).

## 2.4 Electrochemical measurements

Preparation of modified carbon -paste electrode 70% graphite powder, 15% Ag <sub>2</sub>O and 15% silicone oil were hand mixed in a mortar for nearly 30 minutes to produce a homogeneous paste of the modified carbon -paste electrode (MCPE). The cavity of the working electrode was filled with the above prepared paste and was smoothened with a piece of butter paper (B. N. Rashmiet et al., 2019).

## 2.5 Photo catalytic degradation of synthetic textile dyes

Photo catalytic degradation of the commercially used synthetic dyes namely, bromocresolby the Ag<sub>2</sub>O-NPs was observed in the presence of sunlight. About 20 mg of Ag<sub>2</sub>O-NPs was dispersed in 100 mL of an aqueous solution of

Vol 25, No.2 (2024)

http://www.veterinaria.org

Article Received: Revised: Published:



bromocresol(10 mg/L). Visual monitoring and UV-Vis spectroscopic analysis of the mixture were performed at different time intervals. Dye solutions without any NPs were used as respective controls in the study. The degradation percentage was calculated as

 $E(\%) = (C_0 - C_t/C_0) \times 100$ 

where E was the degradation ability,  $C_0$  was the absorbance before irradiation, and  $C_t$  was absorbance at the time (SeerangarajVasantharaj et al.,2021).

#### 2.6 Anticancer activity

Clean the internal surfaces of the gel plates with methylated spirits, dry, and then join the gel plates together to form the cassette, clamp it in a vertical position. In an Erlenmeyer flask or disposable plastic tube, and prepare this parading gel (also called the resolving gel) by mixing the following:

	For15%gels	For10%gels
1.875 Metris-HCl, pH -8.8	8.0ml	8.0ml
Water	11.4ml	18.1ml
Stock acryl amide	20.0ml	13.3ml
10%SDS	0.4ml	0.4ml
Ammonium per sulfate (10%)	0.2ml	0.2ml

De gas this solution under vacuum for about 30sec, Add14ml of TEMED and gently swirl the flask to ensure even mixing. Using a Pasteur pipette transfer this separating gel mixture to the gel cassette carefully down one edge. Continue adding this solution until it reaches a position 1cm from the bottom of the comb that will form the loading well. To ensure that the gel sets with as smooth surface very carefully run distilled water down one edge into the cassette using a Pasteur pipette. While the separating gel is setting prepare the 4% stacking gel solution. Mix the following in a 100ml Erlenmeyer flask or disposable plastic tube.

Chemicals	Amount
0.6 M Tris-Hcl,pH6.8	1.0ml
Stock acryl amide	1.35ml
Water	7.5ml
10%SDS	0.1ml
Stock acryl amide	1.35ml
Ammonium per sulfate	(10%)

0.05ml Degas this solution under vacuum for about 30 sec.When the separating gel has set, pour off the overlaying water. Add 14  $\mu$ l of TEMED to the stacking gel. Pour the stacking gel solution directly onto the surface of the polymerized resolving gel. Immediately insert a clean Teflon comb into the stacking gel solution, being careful to avoid trapping of air bubbles. Place the gel in a vertical position at room temperature and allow to set for 20min.

#### Preparation of samples and running the gel:

About 10ml of protein sample and 5ml of sample buffer are mixed by vortexing. The sample is than heated for 5min at 95-100°C to denature the proteins. The sample is than kept in ice. After polymerization is complete, remove the Teflon comb. Rinse out any unpolymerised acrylamide solution from the wells using electrophoresis buffer and assemble the cassette in the electrophoresis tank. Add Tris-glycine electrophoresis buffer to the top and bottom reservoirs. Load up to 5-10μl of each of the samples (unknown and standard) in a predetermined order into the wells. Connect the electrophoresis apparatus to the power pack (the positive electrode should be connected to the bottom buffer reservoir), and pass a current of 30mA through the gel (constant current) for large format gels, or 200V (constant voltage) for mini gels (Biorad). The gel is run until the bromo phenol blue reaches the bottom of the resolving gel. This will take 2.5-3.0h for large format gels (16μm x 16μm) and about 40min for mini gels (10μm x7μm) (Safety care: Always turnoff & disconnect the power supply before removing the lid). Dismantle the gel apparatus, pry open the gel plates; remove the gel, discard the stacking gel, and place the separating gel in Coomassie blue stain solution. Staining should be carried out with shaking, for a minimum of 2h at room temperature. De stain the gel by soaking it in the acetic acids solution on a slowly rocking plat form for 4-8 hrs. After destaining store the gel sin H<sub>2</sub>O containing 20% glycerol (Kuo-Sheng Hsu et al.,2022).

#### 2.7 Antibacterial Efficiency

The test bacteria was inoculated in peptone water and incubated for 3-4 hours at 35 °C. Mueller hinton agar plates was prepared and poured in sterile petri plates. 0.1 ml of bacterial culture was inoculated on the surface of Mueller hinton



agar plates and spread by using L-rod. The inoculated plates were allowed to dry for five minutes. The disk loaded with Samples concentration  $1000 \mu g/ml$  was placed on the surface of inoculated petri plates using Sterile technique. The plate was incubated at 37 °C for 18-24 hours. The plate was examined for inhibitory zone and the zone of inhibition was measured in mm.(Hudzicki, Jan.,2009)

#### 3. Results and discussions

#### 3.1 Morphological and elemental analysis

SEM micrographs synthesized Ag<sub>2</sub>O-NPs are displayed in Fig1. To optimize the morphology of fabricated Ag<sub>2</sub>O-NPs the extract of *P.indica* and *G,Salicornia* seaweeds concentration were varied. The SEM micrographs of NPs synthesized by using 30 mL and 50 mL of seaweeds extract are depicted in Fig 1a & Fig1 b, respectively. From the SEM micrographs, it is clear that both sample of Ag<sub>2</sub>O-NPs are spherical-like in shape with an average size range of 7.28-7.38nm in *P.indica*, and average size range of 7.71 - 7.94 nm in *G.salicornia*.(El-Ghmari, Brahim, Hanane Farah, and Abdellah Ech-Chahad.,2021)

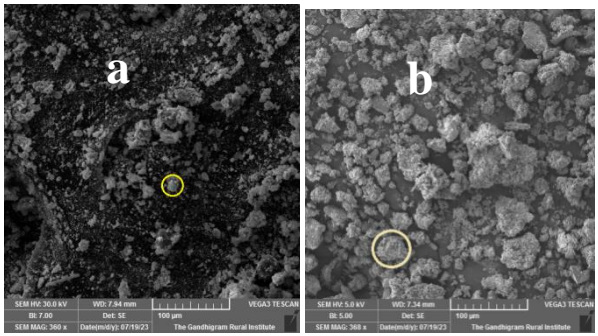


Fig 1:a&b SEM images of Ag<sub>2</sub>O-NPs.using *P.indica* and *G,Salicornia* seaweeds

The elemental composition and purity of synthesized  $Ag_2O$ -NPs were explored using EDAX and spectrum is given in Fig 2a& Fig 2b. The elemental composition and purity of the synthesized silver oxide nanoparticles ( $Ag_2O$ -NPs) were investigated using Energy-dispersive X-ray spectroscopy (EDAX). The EDAX spectrum, as depicted in Fig 2, revealed the presence of peaks solely attributed to silver and oxygen, indicative of pure  $Ag_2O$ -NPs. Notably, there were no discernible peaks corresponding to impurities, affirming the high purity of the synthesized. Table 1a &Table1b showed the amount element present in both seaweeds.

Element		Norm.C [wt.%]	Atom.C [at.%]		Error (3 sigma) [wt.%]
Ag	18.85	62.99	91.98	47	0.40
0	11.08	37.01	8.02	8	3.41
Total	29.93	100.00	100.00		

**Table 1a:** Atomic composition of silver oxide nanoparticles synthesized using *P.indica* whole seaweeds extract.

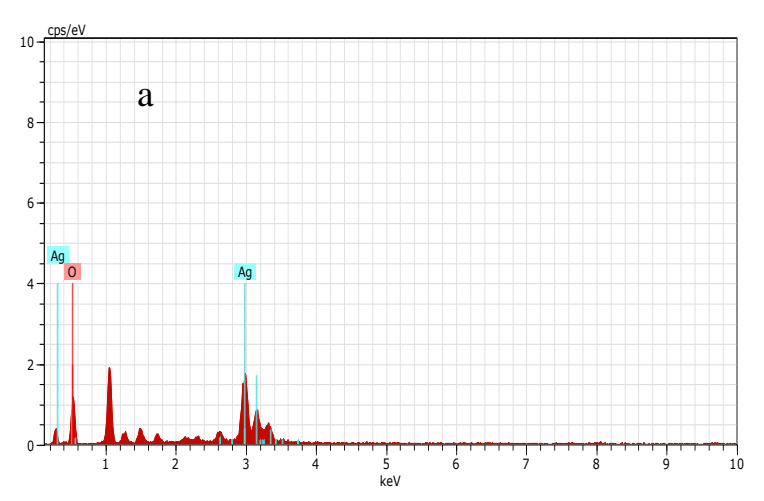


Fig2 a: EDAX Spectrum of silver oxide nanoparticles synthesized using P.indica whole seaweeds extract



Table 1b: Atomic composition of silver oxide nanoparticles synthesized using G.salicornia whole seaweeds extract

Element			Atom.C [at.%]		Error (3 [wt.%]	sigma)
Ag	30.39	89.63	66.18	47	1.04	
O	3.52	10.37	43.82	8	1.50	
Total	31.91	100.00	100.00			

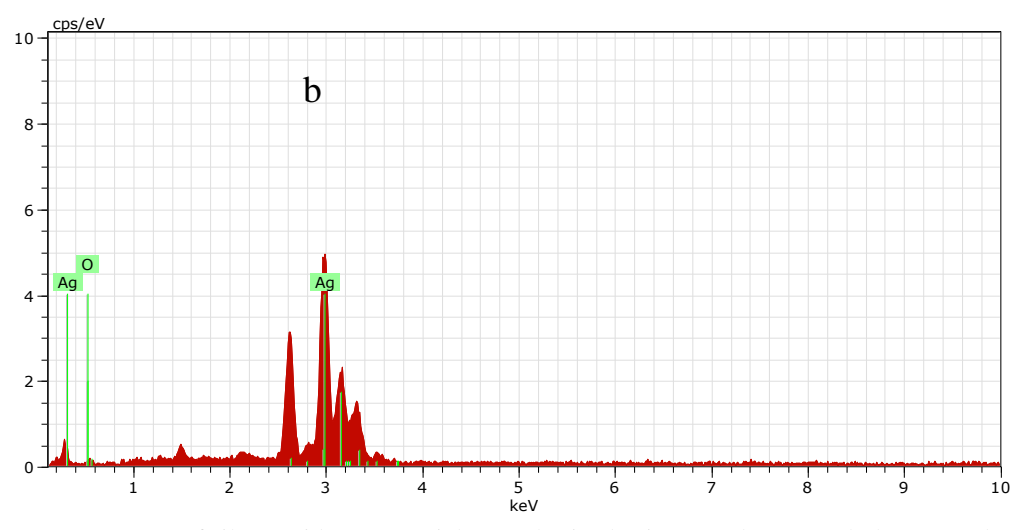


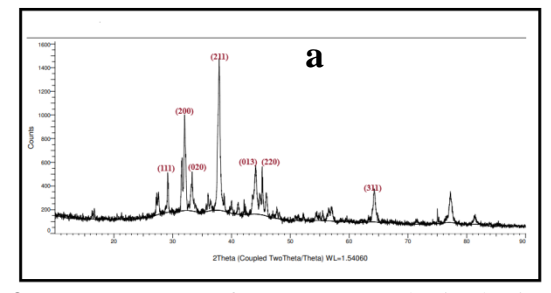
Fig 2b: EDAX Spectrum of silver oxide nanoparticles synthesized using G.salicornia whole seaweeds extract

## 3.2 Structural analysis

The powder XRD crystallography revealed the crystalline nature of the as-synthesized couple of  $Ag_2O$ -NPs. Four major Bragg's reflections at  $29.17^{\circ}$  (111), $31.55^{\circ}$  (200), $40.01^{\circ}$  (211), $43.65^{\circ}$  (013), $47.72^{\circ}$  (220) and  $64.28^{\circ}$  (311) were observed Fig 3a and other seaweeds extract peaks were  $27.51^{\circ}$  (111), $29.16^{\circ}$  (111), $31.90^{\circ}$  (200), $45.869^{\circ}$  (220), $48.16^{\circ}$  (311), $67.01^{\circ}$  (311) were observed Fig 3b respectively. These peaks are well accredited by the standard JCPDS data of the  $Ag_2O$ -NPs of the FCC crystal lattice structure (JCPDS no. 01-1164) respectively Table 2 a & Table 2 b. The average crystallite size of the as-synthesized  $Ag_2O$ -NPs calculated using the Debye–Scherer equation was determined to be 17.7 nm.

Table 2 a&b :XRD parameters of silver oxide Nanoparticles

2θ	FWHM	Size	Plane	2θ	FWHM	Size	Plane
29.17°	0.173	525.7	111	27.51°	0.211	341.7	111
31.55°	0.644	142.6	200	29.16°	0.106	86.1	111
40.01°	0.423	220.8	211	31.90°	0.230	399.2	200
47.72°	0.117	814.4	220	45.86°	0.284	337.7	220
64.28°	0.383	272.2	311	64.28°	0.312	322.5	311



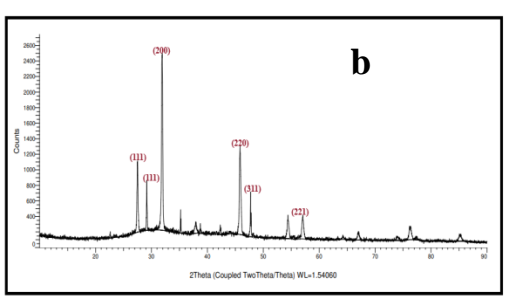


Fig 3 a&b: XRD patterns of Ag<sub>2</sub>O-NPs synthesized using copper sulphate and *P.indica* and *G.salicornia* extract.

#### 3.3 Optical-spectroscopy studies

UV-Vis spectroscopy is an important technique to ensure the formation of metal nanoparticles in aqueous solution. Colour of silver colloidal solution is wine red which is imputed to surface Plasmon resonance (SPR) arising due to the collective oscillation of free conduction electrons induced by an interacting electromagnetic field (Shashanka Rajendrachari et al.,2013). The UV-Vis spectra of the silver oxide nanoparticle obtained. The absorption peak is



plausibly related to the electronic transition taking place from valence band to the conduction band. Peak at 280 nm and 290 nm attribute to the formation of silver oxide showed Fig 4a & Fig 4b nanoparticle. The UV–Vis absorption transition spectrum was used to determine the band gap value of the synthesized Ag<sub>2</sub>O-NPs, which were 2.5 eV and 3.8 eV. This estimation was made using the Tauc plot relation, as shown in Fig 5a & Fig 5b

From the absorption peak the optical energy band gap of Ag<sub>2</sub>O-NPs nano composite has been calculated using the formula

 $E = hc / \lambda$ 

Where h = planck's constant, c = velocity of light, k = wavelength. The band gap energy was calculated as 7.1 eV and 6.8 eV

FTIR analysis were carried out to identify the functional group of the biomolecules present in the red seaweeds are *P. indica* and *G. salicornia* extract which were responsible for the reduction of silver ions and capping of Ag<sub>2</sub>O-NPs. The FTIR spectra depicts the difference in the absorption bands corresponding to the functional molecule present in the red seaweeds extract of *P.indica* and *G. salicornia* Fig. 6a and synthesized Ag<sub>2</sub>O-NPs Fig. 6b. The intense broad band at 3136.84 and 3132.36 cm<sup>-1</sup> represents O-H and C=O stretching modes for the hydroxyl group and stretching bands of the carboxylic acid group,(3300–2500 cm<sup>-1</sup>) and C-H stretching vibration of flavonoids/phenolic group respectively (Debasish Borah et al.,2020). Likewise another band 1559.81cm<sup>-1</sup> due to C=C bending, The medium peak at 1400.90 and 1400.75 cm<sup>-1</sup> represent the C-F stretching-H bending-H bending represent the alcohol as well as polysaccharides .The band at 1041.5 and 1049.7 cm<sup>-1</sup> are attributed to O-Ag-O, while a tri bond of bands at 834,835 and 865.5 cm<sup>-1</sup> are due to stretching vibrations of Ag-O-Ag bond (Amreen Shah et al.,2019).The peaks at 686.7,555 and 563 cm<sup>-1</sup> are represent the C=C bending of alkene, C-Br, C-I stretching like halo compound.The FTIR study revealed that both seaweeds are Ag<sub>2</sub>O-NPs and drug had formed a bridging complex at phenolic oxygen of the moxifloxacin.

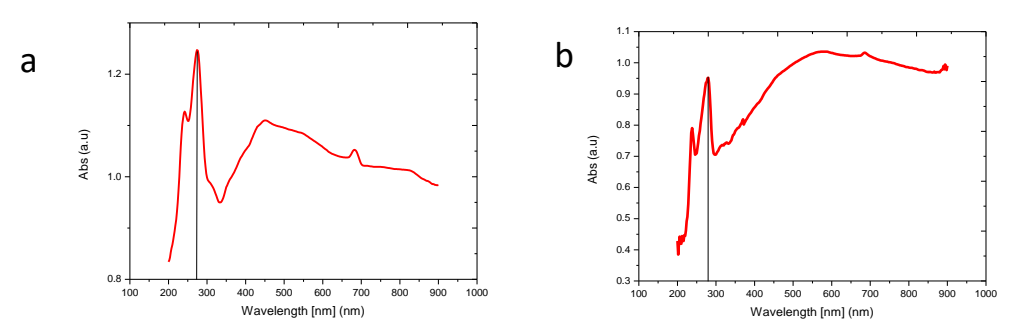


**Fig 4 a&b:** UV–visible spectrum of the Ag<sub>2</sub>O nanoparticles showing absorbance at 280 nm of *P.indica* extract and 290 nm of *G.salicornia* extract

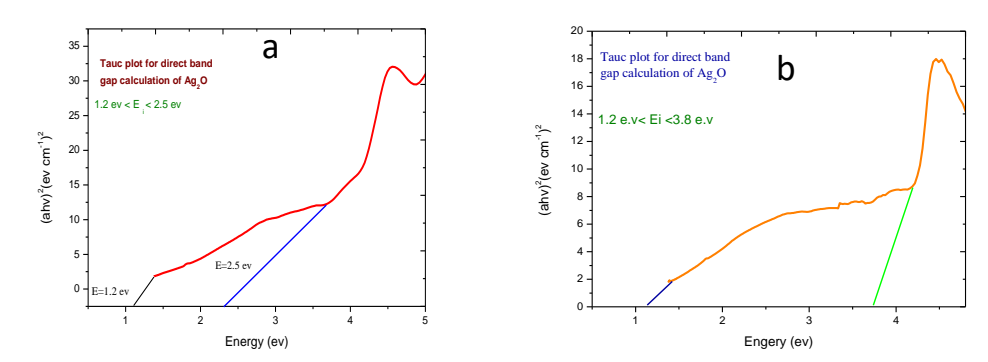


Fig 5 a& b:Tauc plot of Ag<sub>2</sub>O-NPs of *P.indica* extract and *G.salicornia* extract



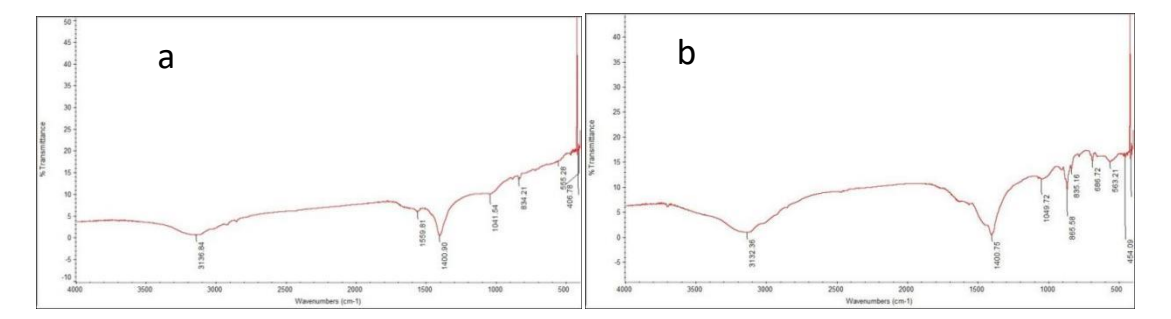


Fig 6 a &b: FTIR analysis for the Ag<sub>2</sub>O nanoparticles showing peaks at various ranges.

#### 4 Applications of Ag<sub>2</sub>O-NPs

 $Ag_2O$ -NPs synthesized using plant extracts have been reported to exhibit numerous applications in many fields. Chemical & Pharmaceutical applications of  $Ag_2O$ -NPs were discussed below as showed in Fig 7 to 11.

#### 4.1 Electro chemical analysis

Cyclic voltammograms of  $Ag_2O$ -NPs were recorded in the potential range from -0.4 to 0.4 V.  $Ag_2O$ -NPs coated on glassy carbon electrode (GCE), Ag/AgCl and platinum wire were used as working, reference and counter electrode, respectively. Fig 7 a & Fig 7 b shows the cyclic voltammogram of Silver oxide at different scan rate of 25mV, 50mV, 75mV, 100mV at produced different cathodic peak and anodic peak was obtained. The voltammogram shows Fig 7a & Fig 7b the oxidation peak observed at 0.18 V and 0.12 V corresponding to the oxidation of  $Ag^0$  to  $Ag^{2+}$  state, when the scan rate increases the cyclic voltammogram curves remain distorted and increase the hump. The reduction peak observed at 0.02 V and -0.02 V, corresponding to the reduction of  $Ag^{2+}$  to  $Ag^0$  state. When the scan rate increases the cyclic voltammogram curves remain distorted, indicating mass transportation and electrode capability (B.S. Narendar et al.,2019).

These results represent the electrochemical behaviour of  $Ag_2O$ -NPs under varying scan rates. The distortions and changes in peak profiles with increasing scan rates highlight the interplay between electron transfer kinetics, diffusion processes, and the capacity of the electrode surface.

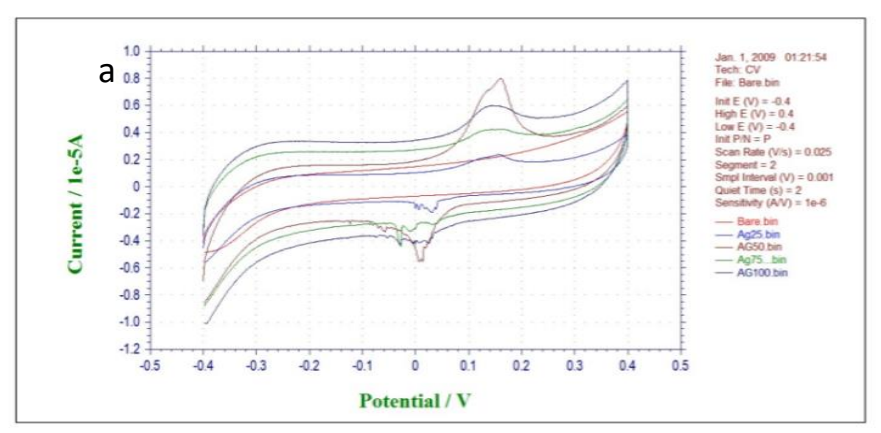


Fig. 7 a: Cyclic voltammetric behaviour of Ag<sub>2</sub>O-NPs at different scan rates using *P.indica* exract

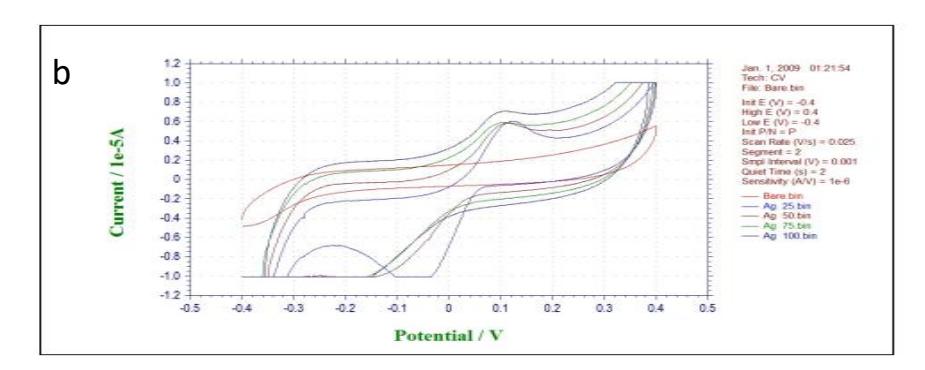


Fig. 7 b: Cyclic voltammetric behaviour of Ag<sub>2</sub>O-NPs at different scan rates using G.slicornia.



#### 4.2 Photocatalytic property

The photocatalytic properties of Ag<sub>2</sub>O nanoparticles synthesized from *Porphyra indica* and *Gracilaria salicornia* were evaluated using aqueous bromocresol purple dye solutions under natural irradiation. During the degradation of the dye, changes in the absorption spectra were observed at 15-minute intervals Fig 8a& Fig 8b. Both seaweed-synthesized Ag<sub>2</sub>O-NPs achieved 70% dye degradation within 2 hours, and extending the process for an additional hour resulted in 100% degradation, as confirmed by the fading of colour Fig. 9.The Ag<sub>2</sub>O-NPs demonstrated a time-dependent photocatalytic activity, effectively degrading bromocresol purple dye.

In general, biological synthesis methods are less toxic than most conventional approaches. The present synthesis method, along with its ability to degrade synthetic dyes, proved more efficient than previously reported studies. The photocatalytic activity of the synthesized Ag<sub>2</sub>O nanoparticles (Ag<sub>2</sub>O-NPs) was found to depend on factors such as particle size, active surface area, oxygen vacancies, and photogenerated carriers, all of which enhance the dye degradation process. Smaller nanoparticles with larger surface areas are particularly effective in generating hydroxyl radicals, thereby increasing photocatalytic activity (SeerangarajVasantharaj et al.,2021).

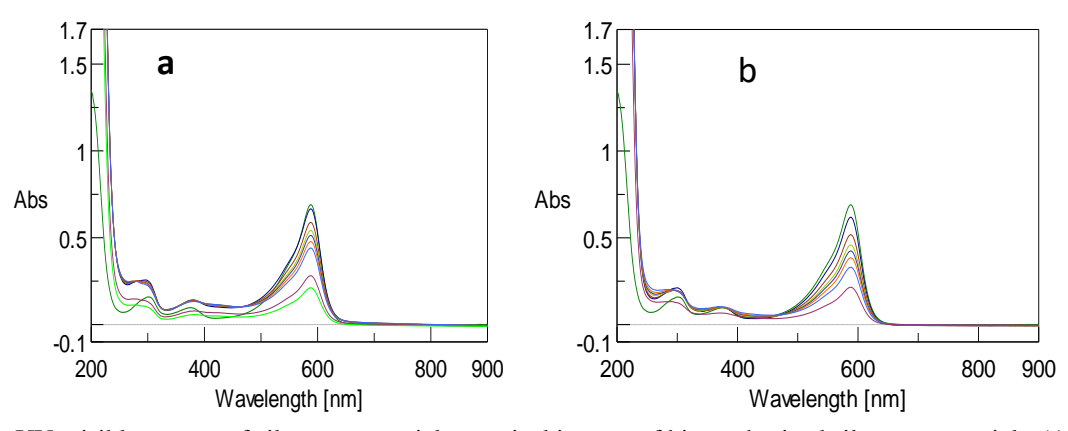


Fig 8a&b: UV-visible spectra of silver nanoparticles, optical images of biosynthesized silver nanoparticles(Ag<sub>2</sub>O-NPs) showing a range of vibrant purple colors from colorless during the course of the reaction using *P.indica&G*.salicornia seaweeds.

In the photocatalytic experiment, a reduction in absorption intensity was observed as the degradation progressed. For  $Ag_2O$ -NPs synthesized from P. indica, the absorption band decreased from 0.661191 nm at 0 minutes to 0.21211 nm after 2 hours. Similarly, for  $Ag_2O$ -NPs synthesized from G. salicornia, the absorption band decreased from 0.611724 nm at 0 minutes to 0.214378 nm after 2 hours. The differences in initial absorption wavelengths between the two samples suggest varying efficiencies in photocatalytic activity, likely due to differences in the source of the silver oxide nanoparticles.



Fig 9: The result of after degradation of bromocresol purple dye in Ag<sub>2</sub>O-NPs of both sea weeds

## 4.3 Antibacterial activity assay by disc diffuse in method

The antimicrobial activity of silver nanoparticles synthesized by natural seaweeds extract was investigated against various pathogenic organisms such as *E. coli,S. aureus ,B. subtilis,B. cereus* and *P. aeruginosa*, using well diffusion method. The diameter of inhibition zones (mm) around each well with silver nanoparticles solution is represented in Table 3.In lower concentration level there was no growth obtained. The silver nanoparticles synthesized by *P. Indica* extracts were found to have highest antimicrobial activity against S. Aureus (9 mm), E. coli (9 mm, at a concentration of 1000  $\mu$ g/ml) (Rajendrachari, Shashanka, et al.,2013,) respectively and the lesser antimicrobial activity of silver nanoparticles were found against *B. cereus*(8mm, at a concentration of 1000  $\mu$ g/ml), *B. subtilis*(8mm, at a concentration of 1000  $\mu$ g/ml) and *P. aeruginosa*(7 mm, at a concentration of 1000  $\mu$ g/ml), and the silver nanoparticles synthesized by *G. Salicornia* extracts were found to have highest antimicrobial activity against *P. aeruginosa*(9 mm, at a concentration



of  $1000 \,\mu g/ml$ ), and the lesser antimicrobial activity of silver nanoparticles were found against E. coli (7 mm, at a concentration of  $1000 \,\mu g/ml$ ), S. aureus(8 mm, at a concentration of  $1000 \,\mu g/ml$ ), B. cereus(8 mm, at a concentration of  $1000 \,\mu g/ml$ ), B. subtilis(8mm, at a concentration of  $1000 \,\mu g/ml$ ) shown in Fig 10 a& Fig 10 b. The silver nanoparticles showed efficient antimicrobial property compared to other salts due to their extremely large surface area, which provides better contact with microorganisms. The nanoparticles get attached to the cell membrane and also penetrated inside the bacteria. The bacterial membrane contains sulphur containing proteins and the silver nanoparticles interact with these proteins in the cell as well as with the phosphorus containing compounds like DNA. When silver nanoparticles enter the bacterial cell it forms a low molecular weight region in the center of the bacteria to which the bacteria conglomerates thus, protecting the DNA from the silver ions. The nanoparticles preferably attack the respiratory chain, cell division finally leading to cell death. The nanoparticles release silver ions in the bacterial cells, which enhance their bactericidal activity (Sondi, I, and Salopek-Sondi, B,2004; Morones, J.R et al.,2005).



**Fig 10 a & b :** Zone of inhibition (mm) against (A) E. coli (B)S. aureus ,(C)B. subtilis,(D) B. cereus and (E) P. aeruginosa respectively to the antimicrobial activity of silver nanoparticles using with P. indica and G. salicornia by discdiffusion and concentration (1000μg/ml) of NPs.

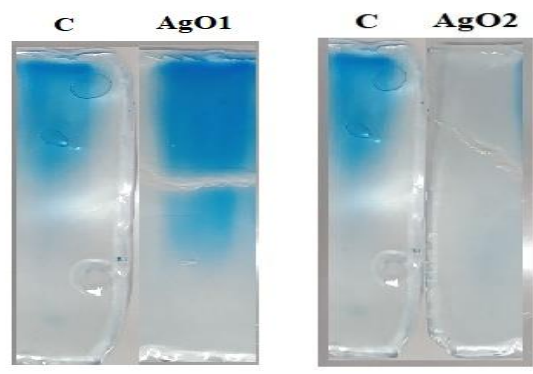
Bacteria	Inhibition zone in mm		Bacteria	Inhibition zone in mm	
	Ab Ampicillin	Ag <sub>2</sub> O of P.i		Ab Ampicillin	Ag <sub>2</sub> O of G.s
E.coli	14	9	E.coli	10	7
Staphylococcus aureus	9	9	Staphylococcus	12	8
			aureus		
Bacillus subtilis	9	8	Bacillus subtilis	16	8
Bacillus cereus	18	8	Bacillus cereus	11	8
Pseudomonas aeruginosa	10	7	Pseudomonas aeruginosa	14	9

Table 3 a&b: Antibacterial growth value of each nanoparticles in P. indica and G.salicornia

#### 4.4. Anti cancer activity by collagen degradation assay

In this given Fig 11, the control lane (Lane C) displays collagen protein without any sample treatment, serving as the baseline for evaluating collagen integrity. The extent of collagen degradation was assessed by analyzing the length of the collagen smear in the gel.Lane 1 and Lane 2 show the effect of Ag<sub>2</sub>O nanoparticles (NPs) synthesized from *G. salicornia*. These lanes demonstrate complete degradation of the collagen, as evidenced by the absence of any staining in the gel. This indicates that the Ag<sub>2</sub>O-NPs from *G. salicornia* exhibit a remarkable ability to break down collagen, which correlates with their high anticancer activity. In comparison, the AgO<sub>1</sub> nanoparticles derived from *P. indica* seaweed show less collagen degradation. This suggests that the anticancer efficacy of Ag<sub>2</sub>O-NPs synthesized from *G. salicornia* is significantly higher compared to those synthesized from *P. indica*.





**Fig 11**: Anticancer activity of collagen degradation assay in AgO-NPs using with *P.indica*, *G.*salicornia seaweeds. The observed high anticancer activity of Ag<sub>2</sub>O-NPs from *G. salicornia* may be attributed to their superior ability to degrade extracellular matrix components like collagen, a crucial step in inhibiting tumor progression and metastasis.

#### Conclusion

Silver oxide nanoparticles ( $Ag_2O$ -NPs) were successfully synthesized using a green, algae-mediated method from P. *indica* and G. *salicornia*seaweeds. This simple, non-toxic process allows for rapid nanoparticle synthesis. The  $Ag_2O$ -NPs from both seaweeds exhibited high photocatalytic degradation activity under visible light. Additionally, they function effectively as electrochemical sensors for uric acid (UA) detection in the presence of dopamine (DA) using cyclic voltammetry, offering a sensitive and selective approach for biological and environmental applications. The antimicrobial study demonstrated that  $Ag_2O$ -NPs possess strong antibacterial properties against B.cereus, E. coli, E0. subtilis, E1. Subtilis, E2. aureus, and E3. Notably, E4. Ag2O-NPs derived from E4. Salicornia were more effective in degrading collagen proteins and exhibited potentially stronger anticancer properties compared to those from E2. Furthermore, the synthesized E4. Ag2O-NPs were stable for over six months without oxide formation, showcasing the method's reliability, eco-friendliness, and cost-effectiveness. These stable E4. Ag2O-NPs hold great potential for applications in medicine, food industries, and sensor technologies, highlighting their wide-ranging utility in both medical and electrochemical sensor fields.

#### References

- 1. Afrin, F., et al. 2023 "Evaluation of antioxidant and antibacterial activities of some selected seaweeds from Saint Martin's Island of Bangladesh." *Food Chemistry Advances* 3 (2023): 100393.
- 2. Aiswarya Devi S, Harshiny M, Udaykumar S, et al (2017) Strategy of metal iron doping and greenmediatedZnO nanoparticles: Dissolubility, antibacterial and cytotoxic traits. Toxicol. Res. 6:854–865. https://doi.org/10.1039/c7tx00093f
- 3. Amreen Shah et al.,2019,Photocatalytic and antibacterial activities of *Paeonia emodi* mediated silver oxide nanoparticles,https://doi.org/10.1088/2053-1591/aafd42
- 4. B. N. Rashmi et al.,(2019),Facile Green synthesis of Silver Oxide Nanoparticles and their Electrochemical, Photocatalytic and Biological Studies, https://doi.org/10.1016/j.inoche.2019.107580
- 5. B.S. Narendar, V. Kumar, M. Tomar, V. Gupta, S.K. Singh, Multifunctional CuO nanosheets for high-performance supercapacitor electrodes with enhanced photocatalytic activity, J. Inorg.Organomet.Polym.Mater.29 (2019) 1067–1075, https://doi.org/10.1007/s10904-018-0995-4.
- 6. Debasish Borah et al.,2020. Alga-mediated facile green synthesis of silver nanoparticles: Photophysical, catalytic and antibacterial activity,https://doi.org/10.1002/aoc.5597
- 7. El-Ghmari, Brahim, Hanane Farah, and Abdellah Ech-Chahad.,2021 "A new approach for the green biosynthesis of Silver Oxide nanoparticles Ag2O, characterization and catalytic application." *Bulletin of Chemical Reaction Engineering & Catalysis* 16.3 (2021): 651-660.
- 8. Franci, G. *et al.* Silver nanoparticles as potential antibacterial agents. *Molecules***20**, 8856-8874.https://doi.org/10.3390/molecules2 0058856 (2015).
- 9. Gurunathan, S., Han, J. W., Kwon, D. N. & Kim, J. H. Enhanced antibacterial and anti-bioflm activities of silver nanoparticles against Gram-negative and Gram-positive bacteria. *Nanosc. Res. Lett.* **9**, 373. https://doi.org/10.1186/1556-276X-9-373 (2014)
- 10. Harshiny Muthukumar et al., 2021, Photocatalytic degradation of caffeine and E. coli inactivation using silver oxide nanoparticles obtained by a facile green co-reduction method, https://doi.org/10.1007/s10098-021-02135-7
- 11. Hudzicki, Jan., 2009 "Kirby-Bauer disk diffusion susceptibility test protocol." *American society for microbiology* 15.1 (2009): 1-23.
- 12. J. M. Zen, A. S. Kumar, and D. M. Tsai, Electroanalysis 15 (2003) 1073. *Anal. Bioanal. Electrochem.*, Vol. 5, No. 4,, 2013, 455 466

REDVET - Revista electrónica de Veterinaria - ISSN 1695-7504

Vol 25, No.2 (2024)

http://www.veterinaria.org

Article Received: Revised: Published:



- 13. J. Saraniya Devi, and B. Valentin Bhimba (2012), Anticancer Activity of Silver Nanoparticles Synthesized by the Seaweed UlvalactucaInvitro, http://dx.doi.org/10.417 2/scientificreports.242
- 14. Kahru A, Dubourguier HC (2010) From ecotoxicology to nanoecotoxicology. Toxicology 269:105–119. https://doi.org/10.1016/j.tox.2009.08.016
- 15. Kuo-Sheng Hsu. et al 2022, Cancer cell survival depends on collagen uptake into tumor-associated stroma, https://doi.org/10.1038/s41467-022-34643-5
- 16. Morones, J.R., Elechiguerra, J.L., Camacho, A., Holt, K., Kouri, J.B., Ramfrez, J.T., Yacaman, M.J., 2005. The bactericidal effect of silver nanoparticles. Nanotechnology 16, 2346–2353.
- 17. Pugazhendhi A, Prabakar D, Jacob JM, et al (2018) Synthesis and characterization of silver nanoparticles using *Gelidiumamansii* and its antimicrobial property against various pathogenic bacteria. Microb.Pathog. 114:41–45. https://doi.org/10.1016/j.micpath.2017.11.013
- 18. Rajendrachari, Shashanka, et al.,2013, "Synthesis of silver nanoparticles and their applications." *Anal. Bioanal. Electrochem* 5.4 (2013): 455-466.
- 19. S. Reddy, B. E. K. Swamy, and H. Jayadevappa, Electrochim. Acta61 (2012) 78.
- 20. S. Reddy, B. E. K. Swamy, B. N. Chandrashekar, S. Chitravathi, and H. Jayadevappa. Anal.Bioanal.Electrochem.4 (2012) 186.
- 21. S. Reddy, B. E. K. Swamy, U. Chandra, B. S. Sherigara, and H. Jayadevappa, Int. J. Electrochem. 5 (2010) 10.
- 22. S. Reddy, B. E. K. Swamy, U. Chandra, K. R. Mahathesha, T. V. Sathish, and H.Jayadevappa, Anal. Met.3 (2011) 2792
- 23. Schröfel A, Kratošová G, Šafařík I, et al (2014) Applications of biosynthesized metallic nanoparticles A review. ActaBiomaterialia 10:4023–4042. https://doi.org/10.1016/j.actbio.2014.05.022
- 24. Seerangaraj Vasantharaj et al 2021, Enhanced photocatalytic degradation of water pollutants using bio-green synthesis of zinc oxide nanoparticles (ZnO NPs), Journal of Environmental Chemical Engineering 9 (2021) 105772, www.elsevier.com/locate/jece.
- 25. Shanmuganathan R, MubarakAli D, Prabakar D, et al (2018) An enhancement of antimicrobial efficacy of biogenic and ceftriaxone-conjugated silver nanoparticles: green approach. Environ. Sci. Pollut. Res.25:10362–10370. https://doi.org/10.1007/s11356-017-9367-9
- 26. Shashanka Rajendrachari et al.,2013, Synthesis of Silver Nanoparticles and their Applications, https://www.researchgate.net/publication/262116441Debasish Borah et,all.,2020 Alga-mediated facile green synthesis of silver nanoparticles: Photophysical, catalytic and antibacterial activity, https://doi.org/10.1002/aoc.5597
- 27. Sondi, I., Salopek-Sondi, B., 2004. Silver nanoparticles as antimicrobial agent: a case study on E. coli as a model for Gram-negative bacteria. J. Colloids Interface Sci. 275, 177–182.
- 28. Vardanyan, Z., Gevorkyan, V., Ananyan, M., Vardapetyan, H. & Trchounian, A. Efects of various heavy metal nanoparticles on *Enterococcus hirae* and *Escherichia coli* growth and proton-coupled membrane transport. *J. Nanobiotechnol.* 13, 69.https://doi. org/10.1186/s12951-015-0131-3 (2015).
- 29. Wang W, Arshad MI, Khurshid M, et al (2018) Antibiotic resistance: a rundown of a globalcrisis. Infect. Drug. Resist. 1645–1658.